



HAL
open science

Impact of episodic vertical fluxes on sea surface pCO₂

Amala Mahadevan, Alessandro Tagliabue, Laurent Bopp, Andrew Lenton,
Laurent Mémery, Marina Lévy

► **To cite this version:**

Amala Mahadevan, Alessandro Tagliabue, Laurent Bopp, Andrew Lenton, Laurent Mémery, et al..
Impact of episodic vertical fluxes on sea surface pCO₂. Philosophical Transactions of the Royal
Society of London. Series A, Mathematical and Physical Sciences (1934–1990), 2011, 369, pp.2009-
2025. 10.1098/rsta.2010.0340 . hal-00634533

HAL Id: hal-00634533

<https://hal.univ-brest.fr/hal-00634533>

Submitted on 16 Feb 2012

HAL is a multi-disciplinary open access archive for the deposit and dissemination of scientific research documents, whether they are published or not. The documents may come from teaching and research institutions in France or abroad, or from public or private research centers.

L'archive ouverte pluridisciplinaire **HAL**, est destinée au dépôt et à la diffusion de documents scientifiques de niveau recherche, publiés ou non, émanant des établissements d'enseignement et de recherche français ou étrangers, des laboratoires publics ou privés.

Impact of episodic vertical fluxes on sea surface pCO₂

BY A. MAHADEVAN¹, A. TAGLIABUE², L. BOPP², A. LENTON³, L. MÉMERY⁴,
M. LÉVY⁵

1. *Department of Earth Sciences, Boston University, Boston, MA, USA*

2. *LSCE-IPSL, CNRS/CEA/UVSQ, Gif-sur-Yvette, France*

3. *CSIRO Wealth from Oceans National Research Flagship, Hobart, TAS, Australia*

4. *LEMAR, UBO/CNRS/IRD, Plouzane, France*

5. *LOCEAN-IPSL, CNRS/UPMC/IRD/MNHN, Paris, France*

Corresponding Author: marina.levy@upmc.fr

15 February 2010

Revised 20 September 2010

ABSTRACT

1

2 Episodic events like hurricanes, storms, and frontal- and eddy-driven upwelling can
3 alter the partial pressure of CO₂ at the sea surface (pCO₂) by entraining subsur-
4 face waters into the surface mixed layer of the ocean. Since pCO₂ is a function of
5 total dissolved inorganic carbon (DIC), temperature (T), salinity (S) and alkalinity
6 (ALK), it responds to the combined impacts of physical, chemical, and biological
7 changes. Here we present an analytical framework for assessing the relative
8 magnitude and sign in the short term perturbation of surface pCO₂ arising from
9 vertical mixing events. Using global, monthly, climatological datasets, we assess
10 the individual, as well as integrated, contribution of various properties to surface
11 pCO₂ in response to episodic mixing. The response depends on the relative vertical
12 gradients of properties beneath the mixed layer. Many areas of the ocean exhibit
13 very little sensitivity to mixing due to the compensatory effects of DIC and T on
14 pCO₂, whereas others, such as the eastern upwelling margins, have the potential
15 to generate large positive/negative anomalies in surface pCO₂. The response varies
16 seasonally and spatially and becomes more intense in subtropical and subpolar re-
17 gions during summer. Regions showing a greater pCO₂ response to vertical mixing
18 are likely to exhibit higher spatial variability in surface pCO₂ on time scales of
19 days.

20 **Keywords:** CO₂, oceanic pCO₂, DIC, sea surface variability, vertical mixing

1. Introduction

21

22 The ocean plays a critical role in mitigating climate change taking up nearly 30%
23 of anthropogenic CO₂ emissions, (Le Quéré *et al.*, 2009). The air-sea flux of CO₂
24 depends on the difference in the partial pressures of CO₂ (pCO₂) between the at-
25 mosphere and sea surface, as well as wind speed and air-sea interfacial conditions,

26 [e.g. Wanninkhof (1992)]. Oceanic surface pCO₂ is a function of dissolved inor-
27 ganic carbon (DIC), temperature (T), salinity (S) and alkalinity (ALK). Hence, it
28 responds to physical processes such as mixing, deep convection, and water mass
29 transformation, as well as biological processes like net primary production (NPP)
30 and remineralization of organic matter. Each of the drivers of oceanic pCO₂ has its
31 own temporal and spatial scales of response to dynamical change. Unsurprisingly,
32 surface pCO₂ is highly variable in space and time, and much of the variability
33 occurs on short timescales (Lenton *et al.*, 2006). Global studies have focussed on
34 understanding the large-scale, seasonal patterns in sea surface pCO₂ and in quan-
35 tifying the related air-sea fluxes of CO₂ at coarse spatial and temporal resolution
36 ($4^{\circ} \times 5^{\circ}$ monthly; Takahashi, *et al.* (2009)). On the other hand, disparate findings
37 have been reported about the variability and controlling factors of surface pCO₂ on
38 short space and time scales (Archer *et al.*, 1996; DeGrandpre *et al.*, 1997; Borges
39 & Frankignoulle, 2001; Copin-Montégut *et al.*, 2004; Körtzinger *et al.*, 2008; Lein-
40 weber *et al.*, 2009; Merlivat *et al.*, 2009), suggesting that there is clearly need for
41 a unified, mechanistic understanding of how surface pCO₂ responds to episodic,
42 localized events that induce vertical mixing.

43 While the surface layer of the ocean is fairly well mixed, there are strong gradi-
44 ents in the vertical distribution of properties beneath the mixed layer (ML). With
45 increasing depth, T decreases, DIC, S and nutrients increase, whereas ALK can in-
46 crease or decrease depending on depth and location. Therefore any physical process
47 that generates localized overturning, up-/down-welling or diapycnal mixing, and
48 entrains water from below the ML, can change the physical-chemical properties
49 in the surface mixed layer. This, along with any subsequent biological changes in
50 response to it, can significantly perturb the mean state of surface pCO₂. We will
51 refer to processes that lead to a vertical flux of properties across the base of the
52 ML, more generally, as “mixing”. Potential mechanisms that can induce such events
53 include negative buoyancy fluxes causing convection, frontal dynamics (Pollard &
54 Regier, 1992; Klein *et al.*, 2008), localized upwelling/mixing due to wind variabil-
55 ity (Hales *et al.*, 2005), storms and hurricanes (Bates *et al.*, 1998), and proposed
56 geo-engineering schemes such as ocean pipes (Lovelock & Rapley, 2007). Indeed the
57 importance of such vertical mixing events on phytoplankton production and the
58 biological pump are now widely recognized (Klein & Coste, 1984; McGillicuddy,
59 Jr. *et al.*, 1998; Mahadevan & Archer, 2000; Lévy *et al.*, 2001, 2009). However,
60 their effect on surface pCO₂ is more complex and difficult to generalize due to the
61 multiple factors that control pCO₂.

62 Several regional studies have examined the short-term response of sea surface
63 pCO₂ to mixing events. Modeling studies of the eastern North Atlantic found lit-
64 tle or no change in the surface pCO₂ in response to upwelling induced by fronts
65 and eddies because additional DIC was counter-balanced by reduced temperature
66 (Mahadevan *et al.*, 2004; Resplandy *et al.*, 2009). Perrie *et al.* (2004) and Bates
67 *et al.* (1998) reported opposing changes in surface pCO₂ in response to hurricane
68 events. These studies highlight the complex interactions of the drivers of oceanic
69 pCO₂ and the difficulty in generalizing the response globally. While global modeling
70 studies (Dutreuil *et al.*, 2009; Yool *et al.*, 2009) that evaluated the ocean pipe geo-
71 engineering schemes examine biological and physical changes due to vertical fluxes,
72 these studies focused on the longer-term impacts through the implementation of a
73 quasi-permanent perturbation to the system. Nevertheless, they also highlight the

74 high degree of spatial variability in the biological and physical response to vertical
75 fluxes.

76 In this study we develop a general theoretical framework, accounting for phys-
77 ical and biological changes in response to mixing, such that the modulation of
78 surface $p\text{CO}_2$ by individual properties, as well as their integrated effect, can be
79 understood on short time scales. The magnitude of the response depends not only
80 on the intensity and duration of the mixing, but also on the location and timing
81 of the events. We quantify the response of surface $p\text{CO}_2$ in terms of the contribu-
82 tions from changes in DIC, T, S and ALK. The sum of these changes can act to
83 either increase or decrease $p\text{CO}_2$. We evaluate these contributions and their inte-
84 gral effect using climatological observations of T, DIC, ALK, nitrate (NO_3) and S.
85 In this study, we apply our framework for assessing short term perturbations from
86 the monthly, mean, climatological distributions. It is complementary to studies of
87 climatological, monthly $p\text{CO}_2$ variability that include the large-scale longer-term
88 response but ignore the short spatial and temporal scale response. It provides a
89 context and mechanistic framework in which differing regional responses can be
90 interpreted. But, the method may also be used with other observational data to
91 examine perturbations arising from specific events on a regional scale.

92 The theoretical framework we present here addresses time scales representative
93 of events lasting up to a few days. We neglect the air-sea exchange of heat, freshwa-
94 ter, and CO_2 in our calculations. Horizontal transport is neglected and only vertical
95 fluxes due to various processes (advective and diapycnal) are represented through
96 a vertical eddy diffusivity acting at the base of the mixed layer. For the sake of this
97 analysis, the MLD and vertical profiles of the oceanic properties (T, DIC, ALK,
98 NO_3) are assumed not to be modified by the vertical mixing. Redfield ratios are
99 used to estimate biological uptake of DIC and only NO_3 is considered as a limiting
100 nutrient (e.g. iron or silicate limitation is neglected). Our analysis relies on using
101 modern (World Ocean Atlas, 2005) climatologies of temperature (Locarnini *et al.*,
102 2006), salinity (Antonov *et al.*, 2006), and NO_3 (Garcia *et al.*, 2006), DIC, and ALK
103 (Key *et al.*, 2004, GLODAP). We realize that these data sets are based on sparse
104 measurements; they may not be reliable in some regions such as the Southern ocean
105 and do not resolve the seasonal variability in DIC and ALK. Our approach is to
106 apply the proposed framework to the best available global data sets in the hope
107 that the broad conclusions are qualitatively correct and will be tested with better
108 data sets in the future. In applying the approach to these data sets, we assume that
109 these large scale properties are not changing with time, apart from changes due to
110 the seasonal cycle that are explicitly or implicitly taken into account in our study.
111 Thus our results only apply for the modern state and ignore inter-annual/decadal
112 variability of ocean properties as well as any long-term trends in those properties.
113 Any long-term changes in mixing or property sources/sinks would alter mean dis-
114 tributions and also bring into effect air-sea fluxes and horizontal circulation. Thus
115 our analysis applies to episodic mixing.

116 2. Theoretical framework

117 To quantify the effect of localized upwelling or vertical mixing on surface $p\text{CO}_2$, we
118 express the rate of change of $p\text{CO}_2$ in terms of the various properties on which it

119 is dependent (Takahashi *et al.*, 1993) as follows

$$120 \quad \frac{\partial \text{pCO}_2}{\partial t} = \frac{\partial \text{pCO}_2}{\partial T} \frac{\partial T}{\partial t} + \frac{\partial \text{pCO}_2}{\partial \text{DIC}} \frac{\partial \text{DIC}}{\partial t} + \frac{\partial \text{pCO}_2}{\partial \text{ALK}} \frac{\partial \text{ALK}}{\partial t} + \frac{\partial \text{pCO}_2}{\partial S} \frac{\partial S}{\partial t}. \quad (2.1)$$

121 In order to consider the response of the surface mixed layer to small-scale upwelling
 122 and/or mixing, we model the vertical flux of any property χ , as a diffusive flux
 123 described by $\kappa \frac{\partial \chi}{\partial z}$, where κ denotes the vertical eddy diffusivity of the property.
 124 This is meant to account for mixing, as well as localized vertical advective fluxes
 125 that occur at horizontal scales much smaller than the resolution of our datasets
 126 (nominally $1^0 \times 1^0$). We therefore assume the value of κ to be the same for all the
 127 properties. The rate of change in any property χ within the ML of depth H , is
 128 modeled as

$$129 \quad \frac{\partial \chi}{\partial t} = -\frac{1}{H} \kappa \frac{\partial \chi}{\partial z} \Big|_{z=-H} + S_\chi. \quad (2.2)$$

130 Here, we consider only a one-dimensional budget for χ to evaluate the effects of
 131 vertical mixing/upwelling. The property χ is assumed to be uniformly mixed within
 132 the ML and any sources/sinks that alter the property in the ML (other than air-sea
 133 fluxes) are denoted by S_χ . Further, $\frac{\partial \chi}{\partial z} \Big|_{z=-H}$ is the vertical gradient across the base
 134 of the mixed layer ($z = -H$) that results in a vertical flux into the ML.

135 We note that the Revelle factors for DIC and ALK, namely,

$$136 \quad \xi = \frac{\Delta \text{pCO}_2}{\text{pCO}_2} / \frac{\Delta \text{DIC}}{\text{DIC}} \Big|_{\text{ALK}=\text{const}} \quad \xi_A = \frac{\Delta \text{pCO}_2}{\text{pCO}_2} / \frac{\Delta \text{ALK}}{\text{ALK}} \Big|_{\text{DIC}=\text{const}} \quad (2.3)$$

137 are variable in space and time with typical values in the range 8–15 for ξ , and -8 –
 138 -13 for ξ_A (Sarmiento & Gruber, 2006). For the salinity and temperature range of
 139 the ocean, there is a well established relationship between pCO_2 and T , as well as
 140 S , (Takahashi *et al.*, 1993)

$$141 \quad \beta = \frac{1}{\text{pCO}_2} \frac{\partial \text{pCO}_2}{\partial T} = 0.0423 \text{ } ^\circ\text{C}^{-1}, \quad \beta_s = \frac{1}{\text{pCO}_2} \frac{\partial \text{pCO}_2}{\partial S} = 0.9^{-1}. \quad (2.4)$$

142 To evaluate the relative change in surface pCO_2 in response to vertical fluxes, we
 143 divide both sides of (2.1) by the value of pCO_2 in the surface layer. Using (2.2)
 144 along with the relationships (2.3) and (2.4), and expressing the time rate of change
 145 of pCO_2 as $\frac{\Delta \text{pCO}_2}{\Delta t}$ we can rewrite (2.1) as

$$146 \quad \frac{\Delta \text{pCO}_2}{\text{pCO}_2} = -\frac{\kappa \Delta t}{H} \left(\beta \frac{\partial T}{\partial z} + \frac{\xi}{\text{DIC}} \frac{\partial \text{DIC}}{\partial z} + \frac{\xi_A}{\text{ALK}} \frac{\partial \text{ALK}}{\partial z} + \beta_S \frac{\partial S}{\partial z} \right) \\ 147 \quad + S_T + S_{\text{DIC}} + S_{\text{ALK}} + S_S. \quad (2.5)$$

148 This equation describes the relative change in surface pCO_2 arising from the in-
 149 dividual responses of DIC, ALK, T and S to vertical mixing across the base of
 150 the mixed layer. All values, other than the gradients, are determined in the mixed
 151 layer. The first four parenthesized terms on the right hand side of (2.5) denote
 152 the relative change in pCO_2 due to the vertical mixing of T , DIC, ALK and S ,
 153 whereas the next four terms denote the relative pCO_2 change due to sources and
 154 sinks for T , DIC, ALK and S . We consider perturbations to the surface pCO_2 due
 155 to vertical oceanic transport alone, while neglecting the atmospheric response, i.e.

156 air-sea fluxes in response to the altered surface pCO₂. In other words, we consider
 157 the perturbation in surface pCO₂ due to episodic oceanic processes, but not the
 158 consequent air-sea equilibration that is expected to occur on longer time scales
 159 (weeks to months) toward neutralizing such perturbations. Surface fluxes of heat,
 160 freshwater and CO₂ are therefore not included. Thus, $S_T = S_S = 0$ and S_{DIC} and
 161 S_{ALK} account for biological effects. More precisely, S_{DIC} accounts for the uptake
 162 of DIC by biological consumption. Vertical mixing and advection supplies remineralized
 163 nutrients to the surface ocean and stimulates NPP. Since NPP is limited by
 164 NO₃ in much of the ocean, we calculate the maximum potential consumption of
 165 DIC during NPP by multiplying the NO₃ supplied through vertical mixing with
 166 the Redfield C/N ratio, $R_{C:N} = 6.625$. To account for light limitation associated
 167 with deepened mixed layers, we multiply the potential DIC consumption by a light
 168 limitation factor $L = 1 - \exp(-E/E_k)$ that varies between 0 and 1 depending on
 169 the mean light availability over the mixed layer. Here E is the climatological mixed
 170 layer average of photosynthetically available radiation (PAR) and E_k is a light limitation
 171 constant taken to be 80 μ -Einsteins m⁻²s⁻¹. The relative change in pCO₂
 172 due to the biological consumption of DIC is thus modeled as

$$173 \quad S_{DIC} = -\frac{\kappa\Delta t}{H} \left(\frac{\xi}{DIC} R_{C:N} L \frac{\partial \text{NO}_3}{\partial z} \right). \quad (2.6)$$

174 The NO₃ that is supplied by mixing, but is left unconsumed by NPP due to light
 175 limitation, contributes alkalinity, which results in a relative change in pCO₂ calculated as

$$177 \quad S_{ALK} = \frac{\kappa\Delta t}{H} \left(\frac{\xi_A}{ALK} \frac{\partial \text{NO}_3}{\partial z} (1 - L) \right). \quad (2.7)$$

178 For much of the ocean, it is reasonable to assume that NO₃ limits biological produc-
 179 tion. However, in the high nutrient low chlorophyll (HNLC) regions of the world's
 180 ocean (primarily the Southern, sub-Arctic Pacific and Equatorial Pacific Oceans),
 181 the micronutrient iron (Fe) limits biological productivity. Taking into account the
 182 limitation of Fe or other potentially limiting nutrients like phosphate or silicic acid
 183 requires knowledge of that nutrient's distribution and the nutrient-specific limita-
 184 tion in phytoplankton production at each location, which we lack and thus do not
 185 include. Similarly, potential changes in species composition and alkalinity consump-
 186 tion during calcification or bacterial remineralization are not accounted for in this
 187 study.

188 3. Datasets and Methods

189 We use a number of different global climatological data sets to evaluate the various
 190 terms in (2.5), which define the contribution of mixing of individual properties on
 191 the relative change in surface pCO₂. Mixed layer depth (MLD), H , based on the
 192 fixed density criterion of 0.03 kg-m⁻³ is taken from the monthly climatology of
 193 de Boyer Montégut *et al.* (2004). To facilitate a common analysis we interpolate all
 194 the data on to the 1⁰ × 1⁰ grid used in the GLObal Ocean Data Analysis Project
 195 (Key *et al.*, 2004, GLODAP). The GLODAP database (Key *et al.*, 2004) provides
 196 an annual mean distribution of DIC and ALK mapped on a 1⁰ × 1⁰ grid globally,
 197 though it should be remembered that the average spacing between the cruises that

198 make up the GLODAP data often exceeds 10^0 . To account for the seasonality in
 199 surface DIC and ALK arising from mixed layer variations, we average the GLODAP
 200 values within the mixed layer, whose depth varies from month to month. This gives
 201 us a monthly, mixed layer DIC and ALK distribution, which includes seasonality
 202 in the MLD, but does not include effects arising from seasonality in biological
 203 production and consumption. Such an approach is justified because the removal
 204 of DIC by biology contributes only a very small perturbation to the total DIC
 205 and its mean profile. Furthermore, a comparison between these monthly DIC and
 206 ALK fields estimated for the ML, and monthly surface DIC and ALK computed
 207 from the surface pCO₂ climatology (Takahashi, et al., 2009) using an empirical
 208 computation of salinity and carbon chemistry (Lenton *et al.*, submitted), reveals
 209 that the differences are insignificant for the purposes of this study.

210 We use monthly values of PAR from the SeaWiFS climatology calculated over
 211 the period 199(7-8) to 2009 (<http://oceancolor.gsfc.nasa.gov/cgi/l3>). This 8km × 8km
 212 resolution monthly data is averaged onto the $1^0 \times 1^0$ grid used in this study. To
 213 account for the small biological response of the austral and boreal winters, we set
 214 the missing values to be 1.25 Einsteins m⁻² day⁻¹. We include the effect of albedo
 215 on PAR by using the monthly mean fractional sea ice cover and assuming that
 216 when sea ice cover exceeds 50%, PAR is reduced by a factor of 0.5. Our value of 0.5
 217 accounts for the combined albedos of open ocean (0.1), sea ice (0.5–0.7) and snow
 218 covered sea ice (0.8–0.9). Climatological values of sea ice are from Walsh (1978)
 219 and Zwally *et al.* (1983). We estimate an average value of PAR for the ML using
 220 Beer’s law for Type 1 waters (Lengaigne *et al.*, 2009) with an e-folding depth scale
 221 of 23m for the attenuation of light downward from the surface.

222 Monthly temperature (Locarnini *et al.*, 2006), salinity (Antonov *et al.*, 2006),
 223 and NO₃ (Garcia *et al.*, 2006) are obtained from the World Ocean Atlas (WOA05)
 224 and regridded on to the GLODAP grid. We average these fields within the mixed
 225 layer for each month to obtain a uniform mixed layer value that we use for consis-
 226 tency with the DIC and ALK fields.

227 To convert the change in DIC and ALK to pCO₂ we use the approximate em-
 228 pirical relationships for Revelle factors of ALK and DIC following Sarmiento &
 229 Gruber (2006); $\xi = \frac{3 \cdot \text{ALK} \cdot \text{DIC} - 2 \cdot \text{DIC}^2}{(2 \cdot \text{DIC} - \text{ALK}) \cdot (\text{ALK} - \text{DIC})}$; $\xi_A = \frac{\text{ALK}^2}{(2 \cdot \text{DIC} - \text{ALK})(\text{ALK} - \text{DIC})}$. We cal-
 230 culate these values monthly to account for seasonal changes in surface DIC and
 231 ALK.

232 The vertical gradients of properties at the base of the mixed layer are derived
 233 by differencing the ML value of the property (described as obtained above) with
 234 the value just beneath the mixed layer on the GLODAP grid. Since MLD varies
 235 from month to month, so do the gradients at the base of the MLD. The evaluation
 236 of vertical gradients in this manner neglects perturbations to the MLD arising from
 237 the localized mixing/upwelling events.

238 In order to compare the relative effects of T, DIC, ALK and the biological
 239 uptake of DIC for a given strength of vertical mixing or upwelling (characterized
 240 by κ) occurring over a time scale representative of synoptic events, we choose $\kappa =$
 241 $10^{-3} \text{m}^2 \text{s}^{-1}$ and $\Delta t = 1$ day in evaluating each of the terms in equation (2.5). Here
 242 κ represents the vertical eddy diffusivity at the base of the mixed layer arising
 243 from mixing (e.g. due to upwelling, wind- or convection-induced overturning or
 244 entrainment), and Δt represents the duration of the episodic mixing event. The

245 specific values of κ would depend on the intensity of the mixing event, strength of
246 stratification and vertical shear at the base of the mixed layer. We do not expect κ
247 to be uniform in time and space, but by choosing a constant value, we are assessing
248 the response of surface $p\text{CO}_2$ to the same intensity of mixing or upwelling applied at
249 any location. The value of Δt is representative of the duration of an episodic mixing
250 event. A larger (or smaller) value of κ or Δt would simply result in an equivalently
251 larger (or smaller) response that can be linearly scaled from the results presented.

252 The relative $p\text{CO}_2$ change due to mixing is estimated globally using the monthly
253 climatological data sets as the sum of various contributions. The physical effects of
254 vertically mixing T, DIC, ALK, S, are cumulatively termed the “abiotic” response,
255 in contrast to the biological response arising from the consumption of DIC in Red-
256 field proportion to the vertically fluxed NO_3 . The increase in alkalinity arising from
257 any excess (unconsumed) NO_3 is also included in the biological response, but is
258 negligible. The effect of salinity perturbations on $p\text{CO}_2$ is negligible compared to
259 the other factors and is not discussed further or presented separately.

260 Before presenting our results, we assess their sensitivity to variations in the
261 MLD. Recomputing the effect of mixing on the relative change in surface $p\text{CO}_2$
262 with the climatological MLD altered by $\pm 20\%$ reveals very little sensitivity to a
263 relative change in MLD. MLD variations are significant only when the ML is shallow
264 ($< 50\text{m}$ in summer). At such times, a large relative perturbation to MLD (which
265 could be small in absolute terms) is required to produce a change in the response.

266 4. Results

267 (a) Varied response of surface $p\text{CO}_2$ to mixing

268 The net response of surface $p\text{CO}_2$ to vertical mixing is highly variable in space
269 and time. Figs. 1a,b are global maps of the relative change in surface $p\text{CO}_2$ arising
270 from mixing during January and July. Mixing of the same intensity ($\kappa =$
271 $10^{-3}\text{m}^2\text{s}^{-1}$) and duration ($\Delta t = 1$ day) is applied globally at the base of the ML
272 to make this assessment. Warm colours (yellow and reds) indicate regions where
273 vertical mixing would enhance the surface $p\text{CO}_2$, whereas cool colours indicate
274 where $p\text{CO}_2$ would be lowered. Large areas of the ocean (coloured in grey or in
275 light shades) show little sensitivity to vertical mixing. While some regions indicate
276 an increase in $p\text{CO}_2$ due to vertical fluxes, others would experience a decrease.
277 Sensitivity to vertical mixing becomes enhanced in stratified regions; hence a much
278 larger response is seen in the hemisphere experiencing summer. This single factor
279 of summertime stratification gives rise to a large seasonality in the response of sur-
280 face $p\text{CO}_2$. A large response is also found on the eastern upwelling margins of the
281 ocean basins. Though we use a colour bar between $\pm 5\%$, the maximum range (for
282 the chosen value of mixing) extends from -27% to $+36\%$. This range, extending
283 from negative to positive, indicates that the same mixing event acting in different
284 locations could elicit a completely opposite response. In some regions, contrasting
285 or opposite tendencies are seen to occur in close proximity of one another. For
286 example, on either side of the Kuroshio and Gulf Stream, and along the eastern
287 equatorial margins, we see alternating positive and negative responses on opposite
288 sides of a front.

289 Figs. 1c,d show the net abiotic response in surface pCO₂. Here, the effects of bi-
 290 ological consumption are not included. Comparison with the panels above (showing
 291 the net effect with biological uptake) reveals that in most regions, biological uptake
 292 does not have a dominant role in modifying the pCO₂ response on these scales.
 293 This is with the exception of some high latitude regions in summer, but the results
 294 are not reliable in the Southern ocean, where NO₃ is known to remain unconsumed
 295 in the surface ocean. When estimating the biological contribution, no time lag is
 296 considered and the biological uptake is assumed to be NO₃ limited.

297 To estimate the absolute change in surface pCO₂ that would result from such
 298 perturbations, we multiply the relative change in pCO₂ by the monthly, climato-
 299 logical surface pCO₂ (Takahashi, et al., 2009). The resulting patterns in surface
 300 pCO₂ variation (Fig. 1e,f) are similar to the relative pCO₂ change (Fig. 1a,b), and
 301 show little or no similarity to the monthly pCO₂ distribution. This suggests that
 302 the pCO₂ response to vertical mixing is governed by the subsurface gradients in the
 303 various properties, and not by the value of the surface pCO₂ per se. The largest vari-
 304 ations in surface pCO₂ occur in the eastern upwelling regions and western boundary
 305 currents, and are in the range of -75 – +60 μatm for the chosen strength of mixing.

306 (b) *Effects of individual properties*

307 To tease apart the contribution of individual factors to the relative change in sur-
 308 face pCO₂, we plot each of the terms in (2.5). These are referred to as the TEM effect
 309 $= -\frac{\kappa\Delta t}{H} \left(\beta \frac{\partial T}{\partial z} \right)$, DIC effect $= -\frac{\kappa\Delta t}{H} \left(\frac{\xi}{\text{DIC}} \frac{\partial \text{DIC}}{\partial z} \right)$, ALK effect $= -\frac{\kappa\Delta t}{H} \left(\frac{\xi_A}{\text{ALK}} \frac{\partial \text{ALK}}{\partial z} \right)$
 310 and BIO effect $= -\frac{\kappa\Delta t}{H} R_{C:N} L \frac{\partial \text{NO}_3}{\partial z}$. The contributions of salinity and S_{ALK} are
 311 small and are not shown. Fig. 2 shows global maps of the remaining factors in
 312 January and July. The effect of DIC is opposite to that of T. While the entrain-
 313 ment of cooler water from subsurface lowers surface pCO₂ (indicated by blue shades
 314 in Fig. 2a,b) the consequent enhancement in surface DIC increases surface pCO₂,
 315 and is consequently shown in yellow and red colours (Fig. 2c,d). A vertical flux of
 316 ALK from the subsurface can either increase or decrease surface pCO₂ according to
 317 whether the vertical gradient in ALK is positive or negative (Fig. 2e,f). The vertical
 318 supply of NO₃ results in an uptake of DIC (lowering pCO₂ as indicated in blue;
 319 Fig. 2g,h), which offsets some of the DIC fluxed in to the ML. Grey regions indicate
 320 a lack of sensitivity of surface pCO₂ to upwelling. The examination of individual
 321 factors explains why one might see a large change in pCO₂ due to upwelling at
 322 certain locations, but not at others.

323 Amongst the various factors, DIC, T and BIO can make a maximum contribu-
 324 tion of about 25% in certain regions, whereas ALK has a smaller range of approxi-
 325 mately ±10%. We would expect the BIO effect to be generally negative since NO₃
 326 increases with depth and mixing causes an enhancement of NO₃ and consumption
 327 of DIC in the ML. But the use of an average value over the ML can sometimes
 328 cause an unphysical reversal of gradient at the base, giving rise to a weak positive
 329 BIO effect in some regions.

330 Fig. 2 indicates that the surface pCO₂ is most responsive to upwelling in the
 331 western boundary systems and coastal upwelling zones. South of the Gulf Stream
 332 and Kuroshio temperature has a controlling effect on pCO₂ variations, such that
 333 surface pCO₂ would be lowered in response to upwelling. North of the Gulf Stream

334 and Kuroshio, DIC has a dominant effect and $p\text{CO}_2$ would increase in response to
335 upwelling. The upwelling region off the west coast of Central America also shows
336 alternating positive and negative perturbations along the coast, with a dominance
337 of the DIC effect off Chile, dominance of the BIO effect off the Peruvian upwelling
338 zone, and DIC dominance further north toward Baja California.

339 Our results suggest that the response of surface $p\text{CO}_2$ to mixing varies region-
340 ally and temporally. Various effects can dominate the $p\text{CO}_2$ perturbation. Fig. 2i,j
341 indicates which effect dominates in a given region during January and July. If the
342 dominant effect does not control the surface $p\text{CO}_2$ variation (i.e. if the response is
343 opposite in sign), we leave the region grey. Since the effects of ALK and salinity
344 are relatively small, the surface $p\text{CO}_2$ is, in general, lowered by upwelling when the
345 effect of T plus biology (BIO) exceeds the effect of upwelled DIC. In most regions of
346 the ocean, the effect of DIC dominates, although BIO and TEM effects do exceed
347 the DIC effect in certain regions. In regions where the temperature or NO_3 effect
348 dominates, $p\text{CO}_2$ will be lowered due to vertical fluxes (assuming the alkalinity
349 effect is negligible).

350 (c) *Seasonally varying response at specific sites*

351 To examine the processes responsible for the seasonal changes in $p\text{CO}_2$ due to
352 localized mixing more closely, Figure 3 presents monthly results for four specific
353 sites, namely the Joint Global Ocean Flux Study (JGOFS) sites of the Bermuda
354 Atlantic Time-Series (BATS) and Hawaii Ocean Time-series (HOT), as well as the
355 North Atlantic Bloom Experiment (NABE site at 47N) and the Antarctic Polar
356 Frontal Zone (APFZ) site. In general, the largest potential changes in $p\text{CO}_2$ arising
357 from localized mixing events occurs in the summer, when the mixed layer is shal-
358 lowest and the gradients at its base are sharpest. In the wintertime, deep mixed
359 layers result in a relatively homogenous water column and the impacts of mixing are
360 thus minimized. Nevertheless, it is also important to note that the degree of density
361 stratification is greatest during the summer, which may make it more difficult to
362 obtain a large vertical flux.

363 If we first examine the subtropical stations BATS and HOT, we find that al-
364 though the DIC effect consistently increases $p\text{CO}_2$ year round (Fig. 3), the impact
365 of temperature is different between the two sites. The TEM effect contributes a
366 large reduction in $p\text{CO}_2$ during the summertime at BATS, whereas it makes vir-
367 tually no contribution at HOT. This is because the thermocline is much sharper
368 and shallower at BATS relative to HOT (for example between 0 and 100m, Fig. 3),
369 which leads to a greater cooling of surface waters and hence a reduction in $p\text{CO}_2$
370 in response to localized mixing. The impact of biological production at both sites
371 is of little consequence, because the nitricline is consistently deeper than the mixed
372 layer (i.e., the depth across which anomalous mixing occurs, Figure 3). Accordingly,
373 at BATS, the TEM effect (and to a lesser extent the ALK effect) can more than
374 offset the increased $p\text{CO}_2$ due to DIC in summer and mixing contributes to a net
375 reduction in $p\text{CO}_2$ between May and August. At HOT, the TEM effect is too weak
376 to counter-balance the DIC effect and mixing results in a small relative increase in
377 $p\text{CO}_2$.

378 At the high latitude stations (NABE and APFZ) there is a great deal of sea-
379 sonality. At NABE, mixing has little impact during the winter, since mixed layers

380 are already very deep (>200m). In the spring and summertime, mixing of DIC in-
381 creases pCO₂ greatly and the counter-balancing effect of temperature is not as large
382 as at BATS. Hence, the net effect of all abiotic processes results in a net increase
383 in pCO₂ in response to localized mixing between March and November (Fig. 3).
384 However, the biological effect during the spring to autumn period is much larger
385 than at BATS or HOT, because the nitricline is much shallower, and is thus almost
386 able to offset the net effect of abiotic processes for much of the spring and summer.
387 Including the impact of biology means that mixing actually leads to a net reduc-
388 tion in pCO₂ during September and October (Figure 3). However, it is important
389 to note that biology needs to act in concert with T to drive the reduction in pCO₂
390 during this period. The APFZ similarly shows large changes throughout the year.
391 As seen previously, mixing of DIC causes large increases in pCO₂ even in the winter
392 (as winter mixed layers are shallower than at NABE). This is offset slightly by the
393 combination of the smaller effects of T and ALK during the spring and summer,
394 but still results in a net increase in pCO₂ due to abiotic processes. Localised mixing
395 causes a large net reduction in pCO₂ between November and March. This is due to
396 a large increase in biological productivity associated with the increased vertical flux
397 of NO₃ that can more than counter balance the net increase in pCO₂ associated
398 with abiotic processes. However, the BIO effect might be over estimated in the iron
399 limited APFZ if the ferricline were deeper than the nitricline. The biological re-
400 sponse to a localized mixing event is based on the NO₃ profile and assumes a fixed
401 C/N ratio. However, increasing the supply of iron to phytoplankton results in a
402 concomitant increase in their demand for iron (Sunda & Huntsman, 1997; Dutreuil
403 *et al.*, 2009). This would be translated into a reduction in the C/Fe ratio in response
404 to an increased vertical flux of iron associated with a localized mixing event. As
405 such, our results regarding the biological response should be seen as maximal effects
406 in the iron limited Southern Ocean.

407 Overall, we find that there are often compensatory processes that act in concert
408 to moderate or enhance the response of surface pCO₂ to localized mixing on a
409 month by month basis. While DIC always drives an increase in surface pCO₂, T
410 and/or BIO are able to compensate for this effect during the summertime and cause
411 a net reduction in pCO₂ at some stations. Biology is generally weak in the tropics
412 and T can cause a seasonal reduction in pCO₂ at BATS, but not at HOT. This is
413 due to variability in the thermocline depth, relative to the depth of mixing between
414 each station. On the other hand, the TEM effect is weaker at high latitudes (NABE
415 and APFZ) and biological activity is the predominant means by which the impact
416 of DIC is offset to cause a net pCO₂ reduction in summer. The combination of T
417 and BIO is more important at NABE than at APFZ, although we note that the
418 BIO effect might be overestimated at APFZ.

419 5. Discussion

420 The proposed framework allows us to synthesize the findings of several recent stud-
421 ies that have examined the response of the surface ocean to upwelling or mixing
422 events. Bates *et al.* (1998) found that in the Sargasso sea, the surface ocean cooled
423 by several degrees with the passing of hurricane Felix in 1995. The lowered tempera-
424 ture affected the surface pCO₂, which was lowered by 60 μ atm. A similar effect was
425 reported by Koch *et al.* (2009). This is consistent with our analysis (Fig. 2, right

426 column) which shows that in the region of the Sargasso Sea, the effect of tempera-
427 ture (TEM effect) dominates the change in surface $p\text{CO}_2$ induced by mixing during
428 summer. Further to the north (at 72.5W, 39.5N), the passage of extra-tropical
429 hurricane Gustav (2002) caused no significant cooling, but an increase sea surface
430 $p\text{CO}_2$ of $50\mu\text{atm}$ due to the enhancement of DIC (Perrie *et al.*, 2004). This too is
431 consistent with Fig. 1 and Fig. 2, which show the dominance of the DIC effect and
432 potential increase in $p\text{CO}_2$ due to mixing in this region over the summer.

433 Modeling studies that were based on conditions in the North Atlantic during
434 the summer (Mahadevan *et al.*, 2004), as well as winter (Resplandy *et al.*, 2009),
435 revealed that upwelling induced by fronts and eddies generates little or no change in
436 the surface $p\text{CO}_2$. This is consistent with our results, since we find that the change
437 in $p\text{CO}_2$ in the NE Atlantic is negligible in January (Fig. 1a) and less than $5\mu\text{atm}$
438 in July, largely because the effects of lowered T and increased DIC negate each
439 other. The largest changes in the North Atlantic are actually found on the western
440 side, north of the Gulf Stream in January and on either side of the Gulf Stream
441 in July, due to stronger DIC gradients. However, it should be noted that impacts
442 of submesoscale dynamics on surface $p\text{CO}_2$ do not only include vertical processes.
443 Both modeling studies have indeed revealed very clearly that lateral stirring by
444 mesoscale eddies of surface water masses with substantially different $p\text{CO}_2$ gener-
445 ates strong gradients in surface $p\text{CO}_2$, in agreement with those observed in the
446 field (Watson *et al.*, 1991; Resplandy *et al.*, 2009). This effect, not considered here,
447 mainly redistributes $p\text{CO}_2$ at small spatial scales without significantly modifying
448 its mean value, which is not the case when vertical fluxes are involved.

449 There are some important implications for the response of surface $p\text{CO}_2$ to
450 episodic vertical fluxes. Regions and times that show a large sensitivity of surface
451 $p\text{CO}_2$ to vertical mixing can be expected to exhibit greater spatial and temporal
452 variance in surface $p\text{CO}_2$, which has consequences for calculating carbon budgets
453 (Monteiro *et al.*, 2009). Secondly, changes in $p\text{CO}_2$ are concomitant with a change in
454 seawater pH, or ocean acidification. Thus, this analysis helps to identify regions that
455 would be particularly vulnerable to changes in pH, such as the west coast of North
456 America where marine ecosystems could be at stake (Feely *et al.*, 2008). On the
457 other hand, we expect that the impact of mixing-induced perturbations in surface
458 $p\text{CO}_2$ on large-scale air-sea CO_2 fluxes would be negligible due to the limited area
459 and duration of the $p\text{CO}_2$ modulations (Lenton *et al.*, 2006). In some instances,
460 however, as in the case of hurricanes, a systematic correlation with higher wind
461 speeds and gas exchange rates could enhance the sea-to-air gas flux as reported by
462 Bates *et al.* (1998).

463 Estimates of the BIO effect in this framework should be viewed with some
464 caution. Our present results indicate that the effect of DIC broadly dominates
465 the $p\text{CO}_2$ perturbation, and that vertically fluxed NO_3 does not account for the
466 complete consumption (in Redfield proportion) of vertically fluxed DIC. In reality,
467 the biological response to the vertical flux of nutrients is complex, depending on
468 species composition, micro nutrients, variable stoichiometric ratios and variability in
469 PAR. Thus it is often difficult to capture the biological response even with ecosystem
470 models, and the simplistic approach taken here may very well underestimate the
471 biological contribution. Furthermore, we point out the potential for inconsistencies
472 amongst the data sets used in this study since they are constructed from varied
473 sources of data with different methods.

474 In the future, with climate change, we would expect an increase in surface ocean
 475 temperatures and vertical gradients in temperature. Consequently, the negative
 476 perturbation of T on pCO₂ due to mixing (TEM effect) would be enhanced, even
 477 as surface pCO₂ is likely to be higher due to higher surface T and DIC. Increasing
 478 surface DIC due to the uptake of anthropogenic CO₂ will reduce the positive effect
 479 of DIC on surface pCO₂ in response to mixing. Using the GLODAP data, we can
 480 estimate that the vertical gradient in DIC (between the surface and depths of 100m–
 481 300m) has already declined by 5-10% since the pre-industrial. Thus, the net effect
 482 is likely to be a reduction in the dominance of the DIC effect and increase in the
 483 dominance of the TEM effect, tending to decrease the surface pCO₂ perturbation
 484 (or make it more negative) in response to mixing. However, the effects of subduction
 485 and circulation are known to complicate this simple picture by sequestering more
 486 anthropogenic CO₂ at depth than at the surface in some locations. It is also likely
 487 that climate change will modify the degree of stratification (Sarmiento *et al.*, 2004),
 488 which may impact the strength and frequency of episodic mixing events in the
 489 future.

490 6. Conclusions

491 We propose an analytical framework that we apply to observational datasets for
 492 analyzing the impact of vertical fluxes in DIC, ALK, T, S and NO₃ on sea surface
 493 pCO₂. We make a global, monthly, assessment of the surface pCO₂ perturbations
 494 due to episodic mixing of a given strength. We find a great deal of spatial and
 495 temporal variability in the pCO₂ response at the sea surface, with the amplitude
 496 of the perturbation exceeding 20μatm in many regions, and being positive in some
 497 areas and negative in others. The largest surface pCO₂ response to vertical mixing
 498 is found in eastern upwelling margins and regions with shallow mixed layers during
 499 the summer. The response depends on the interactive effects of DIC, T, ALK and
 500 biology, which can compensate or reinforce their individual effects. This explains
 501 why a given mixing event (e.g., the passage of a hurricane or vertical advection from
 502 frontogenesis) can elicit an increase or a decrease in surface pCO₂ depending on
 503 its precise location and timing. In general, entrainment of DIC from the subsurface
 504 increases surface pCO₂, while a reduction in T and the biological uptake of DIC
 505 act to reduce pCO₂. The response due to ALK is spatially variable. In the future,
 506 climate change will likely modify the oceanic mean vertical gradients of temper-
 507 ature and DIC due to the uptake of anthropogenic CO₂, thereby reducing pCO₂
 508 perturbations and variability arising from vertical mixing, even as the mean surface
 509 pCO₂ may be higher.

510 **Acknowledgements:** A.M. acknowledges support from NASA grant NNX08AL80G, and
 511 A.L. from the Australian Climate Change Science Program.

512 References

- 513 Antonov, J., Locarnini, R., Boyer, T., Mishonov, A. & Garcia, H. 2006 World Ocean
 514 Atlas 2005, Volume 2: Salinity. Tech. rep., NOAA Atlas NESDIS 62, U.S. Government
 515 Printing Office, Washington, D.C., 182 pp.
- 516 Archer, D., Takahashi, T., Sutherland, S., Goddard, J., Chipman, D., Rodgers, K. &
 517 Ogura, H. 1996 Daily, seasonal and interannual variability of sea-surface carbon and

- 518 nutrient concentration in the equatorial Pacific Ocean. *Deep Sea Res. II Topical Studies*
519 *in Oceanogr.*, **43**(4-6), 779–808.
- 520 Bates, N., Knap, A. & Michaels, A. 1998 Contribution of hurricanes to local and global
521 estimates of air-sea exchange of CO₂. *Nature*, **395**, 58–61. (doi:10.1038/25703)
- 522 Borges, A. & Frankignoulle, M. 2001 Short-term variations of the partial pressure of CO₂
523 in surface waters of the Galician upwelling system. *Prog. Oceanogr.*, **51**, 283–302.
- 524 Copin-Montégut, C., Bégovic, M. & Merlivat, L. 2004 Variability of the partial pressure of
525 CO₂ on diel to annual time scales in the northwestern Mediterranean Sea. *Mar. Chem.*,
526 **85**, 169–189.
- 527 de Boyer Montégut, C., Madec, G., Fischer, A., Lazar, A. & Iudicone, D. 2004 Mixed
528 layer depth over the global ocean: an examination of profile data and a profile-based
529 climatology. *J. Geophys. Res.*, **109**(C12003). (doi:10.1029/2004JC002378)
- 530 DeGrandpre, M., Hammar, T., Wallace, D. & Wirick, C. 1997 Simultaneous mooring-based
531 measurements of seawater CO₂ and O₂ off Cape Hatteras, North Carolina. *Limnol.*
532 *Oceanogr.*, **42**, 21–28.
- 533 Dutreuil, S., Bopp, L. & Tagliabue, A. 2009 Impact of enhanced vertical mixing on marine
534 biogeochemistry: Lessons for geo-engineering and natural variability. *Biogeosciences*, **6**,
535 901–912.
- 536 Feely et al., R. 2008 Evidence for upwelling of corrosive “acidified” water onto the conti-
537 nental shelf. *Science*, **320**(5882), 1490–1492. (doi:10.1126/science.1155676)
- 538 Garcia, H. E., Locarnini, R. A., Boyer, T. P. & Antonov, J. 2006 World Ocean Atlas 2005,
539 Volume 4: Nutrients (phosphate, nitrate, silicate). Tech. rep., NOAA Atlas NESDIS
540 64, U.S. Government Printing Office, Washington, D.C., 396 pp.
- 541 Hales, B., Takahashi, T. & Bandstra, L. 2005 Atmospheric CO₂ uptake by a coastal up-
542 welling system. *Global Biogeochem. Cycles*, **19**(GB1009). (doi:10.1029/2004GB002295)
- 543 Key, R., Kozyr, A., Sabine, C., Lee, K., Wanninkhof, R., Bullister, J., R.A. Feely, F. M.,
544 Mordy, C. & Peng, T.-H. 2004 A global ocean carbon climatology: Results from GLO-
545 DAP. *Global Biogeochem. Cycles*, **18**, GB4031.
- 546 Klein, P. & Coste, B. 1984 Effects of wind-stress variability on nutrient transport into the
547 mixed layer. *Deep Sea Res., A*, **31**, 21–37.
- 548 Klein, P., Hua, B. L., Lapeyre, G., Capet, X., Le Gentil, S. & Sasaki, H. 2008 Upper ocean
549 turbulence from high-resolution 3-D simulations. *J. Phys. Oceanogr.*, **38**, 1748–1763.
- 550 Koch, J., McKinley, G., Bennington, V. & Ullman, D. 2009 Do hurricanes cause signifi-
551 cant interannual variability in the air-sea CO₂ flux of the subtropical North Atlantic?
552 *Geophys. Res. Lett.*, **36**, L07606. (doi:10.1029/2009GL037553)
- 553 Körtzinger, A., Send, U., Lampitt, R., Hartman, S., Wallace, D., Karstensen, J., Villagar-
554 cia, M., Llinás, O. & DeGrandpre, M. 2008 The seasonal pCO₂ cycle at 49°N 16.5°W
555 in the northeastern Atlantic ocean and what it tells us about biological productivity.
556 *J. Geophys. Res.*, **113**(C04020). (doi:10.1029/2007JC004347)
- 557 Le Quééré, C., Raupach, M., Canadell, J. & et al., G. M. 2009 Trends in the sources and
558 sinks of carbon dioxide. *Nature Geoscience*, **2**, 831–836. (doi:10.1038/ngeo689)

- 559 Leinweber, A., Gruber, N., Frenzel, H., Friederich, G. & Chavez, F. 2009 Diurnal carbon
560 cycling in the surface ocean and lower atmosphere of Santa Monica Bay, California.
561 *Geophys. Res. Lett.*, **36**, L08 601. (doi:10.1029/2008GL037018)
- 562 Lengaigne, M., Madec, G., Bopp, L., Menkes, C., Aumont, O. & Cadule, P. 2009 Bio-
563 physical feedbacks in the Arctic Ocean using an earth system model. *Geophys. Res.*
564 *Lett.*, **36**(L21602). (doi:10.1029/2009GL040145)
- 565 Lenton, A., Matear, R. & Tilbrook, B. 2006 Design of an observational strategy for
566 quantifying the Southern Ocean uptake of CO₂. *Global Biogeochem. Cycles*, **20**. (doi:
567 10.1029/2005GB002620)
- 568 Lenton, A., Metzl, N., Takahashi, T., Sutherland, S., Tilbrook, B., Kuchinke, M. &
569 Sweeney, C. submitted The observed evolution of the trends and drivers of oceanic
570 pCO₂ over the last two decades. *Global Biogeochem. Cycles*.
- 571 Lévy, M., Klein, P. & Jelloul, M. B. 2009 New production stimulated by high-frequency
572 winds in a turbulent mesoscale eddy field. *Geophys. Res. Lett.*, **36**(16), L16 603.
- 573 Lévy, M., Klein, P. & Treguier, A. M. 2001 Impacts of sub-mesoscale physics on production
574 and subduction of phytoplankton in an oligotrophic regime. *J. Mar. Res.*, **59**, 535–565.
- 575 Locarnini, R., Mishonov, A., Antonov, J., Boyer, T. & Garcia, H. 2006 World Ocean Atlas
576 2005, Volume 1: Temperature. Tech. rep., NOAA Atlas NESDIS 61, U.S. Government
577 Printing Office, Washington, D.C., 182 pp.
- 578 Lovelock, J. & Rapley, C. G. 2007 Ocean pipes could help the earth to cure itself. *Nature*,
579 **447**, 403.
- 580 Mahadevan, A. & Archer, D. 2000 Modeling the impact of fronts and mesoscale circulation
581 on the nutrient supply and biogeochemistry of the upper ocean. *J. Geophys. Res.*,
582 **105**(C1), 1209–1225.
- 583 Mahadevan, A., Lévy, M. & Mémerly, L. 2004 Mesoscale variability of sea sur-
584 face pCO₂: What does it respond to? *Global Biogeochem. Cycles*, **18**(1),
585 GB101 710.10292003GB002 102.
- 586 McGillicuddy, Jr., D., Robinson, A., Siegel, D., Jannasch, H., Johnson, R., Dickey, T., Mc-
587 Neil, J., Michaels, A. & Knap, A. 1998 Influence of mesoscale eddies on new production
588 in the Sargasso Sea. *Nature*, **394**, 263–266.
- 589 Merlivat, L., Davila, M. G., Caniaux, G., Boutin, J. & Reverdin, G. 2009 Mesoscale and diel
590 to monthly variability of CO₂ and carbon fluxes at the ocean surface in the northeastern
591 Atlantic. *J. Geophys. Res.*, **114**(C3), C03 010. (doi:10.1029/2007JC004657)
- 592 Monteiro et al., P. 2009 A global sea surface carbon observing system: Assessment of
593 changing sea surface CO₂ and air-sea CO₂ fluxes. Tech. rep., OceanObs Community
594 White Paper, 1-25 September 2009, Venice, Italy.
- 595 Perrie, W., Zhang, W., Ren, X., Long, Z. & Hare, J. 2004 The role of midlatitude storms on
596 air-sea exchange of CO₂. *Geophys. Res. Lett.*, **31**, L09 306. (doi:10.1029/2003GL019212)
- 597 Pollard, R. & Regier, L. 1992 Vorticity and vertical circulation at an ocean front. *J. Phys.*
598 *Oceanogr.*, **22**, 609–625.

- 599 Resplandy, L., Lévy, M., dOvidio, F. & Merlivat, L. 2009 Impact of submesoscale
600 variability in estimating the air-sea CO_2 exchange: Results from a model study of
601 the POMME experiment. *Global Biogeochem. Cycles*, **23**(GB1017), 19pp. (doi:
602 10.1029/2008GB003239)
- 603 Sarmiento, J. & Gruber, N. 2006 *Ocean biogeochemical dynamics*. Princeton University
604 Press, Princeton, USA.
- 605 Sarmiento, J., Slater, R., Barber, R., Bopp, L., Doney, S., Hirst, A., Kleypas, J., Matear,
606 R., Mikolajewicz, U. *et al.* 2004 Response of ocean ecosystems to climate warming.
607 *Global Biogeochem. Cycles*, **18**(GB3003). (doi:10.1029/2003GB002134)
- 608 Sunda, W. & Huntsman, S. 1997 Interrelated influence of iron, light and cell size on marine
609 phytoplankton growth. *Nature*, **390**, 389–392.
- 610 Takahashi, T., Olafsson, J., Goddard, J., Chipman, D. & Sutherland, S. C. 1993 Seasonal
611 variation of CO_2 and nutrients in the high-latitude surface oceans: A comparative study.
612 *Global Biogeochem. Cycles*, **7**(4), 843–878.
- 613 Takahashi, et al. 2009 Climatological mean and decadal change in surface ocean $p\text{CO}_2$,
614 and net sea-air CO_2 ux over the global oceans. *Deep Sea Res. II*, **56**, 554577. (doi:
615 10.1029/2004JC002378)
- 616 Walsh, J. 1978 A data set on northern hemisphere sea ice extent, 1953-1976. Tech. Rep.
617 Report GD-2, 49-51, World Data Center for Glaciology (Snow and Ice).
- 618 Wanninkhof, R. 1992 Relationship between wind speed and gas exchange over the ocean.
619 *J. Geophys. Res.*, **97**(C5), 7373–7382.
- 620 Watson, A., Robinson, C., Robinson, J., B. Williams, P. L. & Fasham, M. 1991 Spatial
621 variability in the sink for atmospheric carbon dioxide in the North Atlantic. *Nature*,
622 **350**, 50–53.
- 623 Yool, A., Shepherd, J., Bryden, H. & Oschlies, A. 2009 Low efficiency of nutrient translo-
624 cation for enhancing oceanic uptake of carbon dioxide. *J. Geophys. Res.*, **114**(C08009).
625 (doi:10.1029/2008JC004792)
- 626 Zwally, H., Comiso, J., Parkinson, C., Campbell, W., Carsey, F. & Gloerson, P. 1983
627 Antarctic sea ice, 1973-1976: Satellite passive microwave observations. Tech. rep.,
628 NASA.

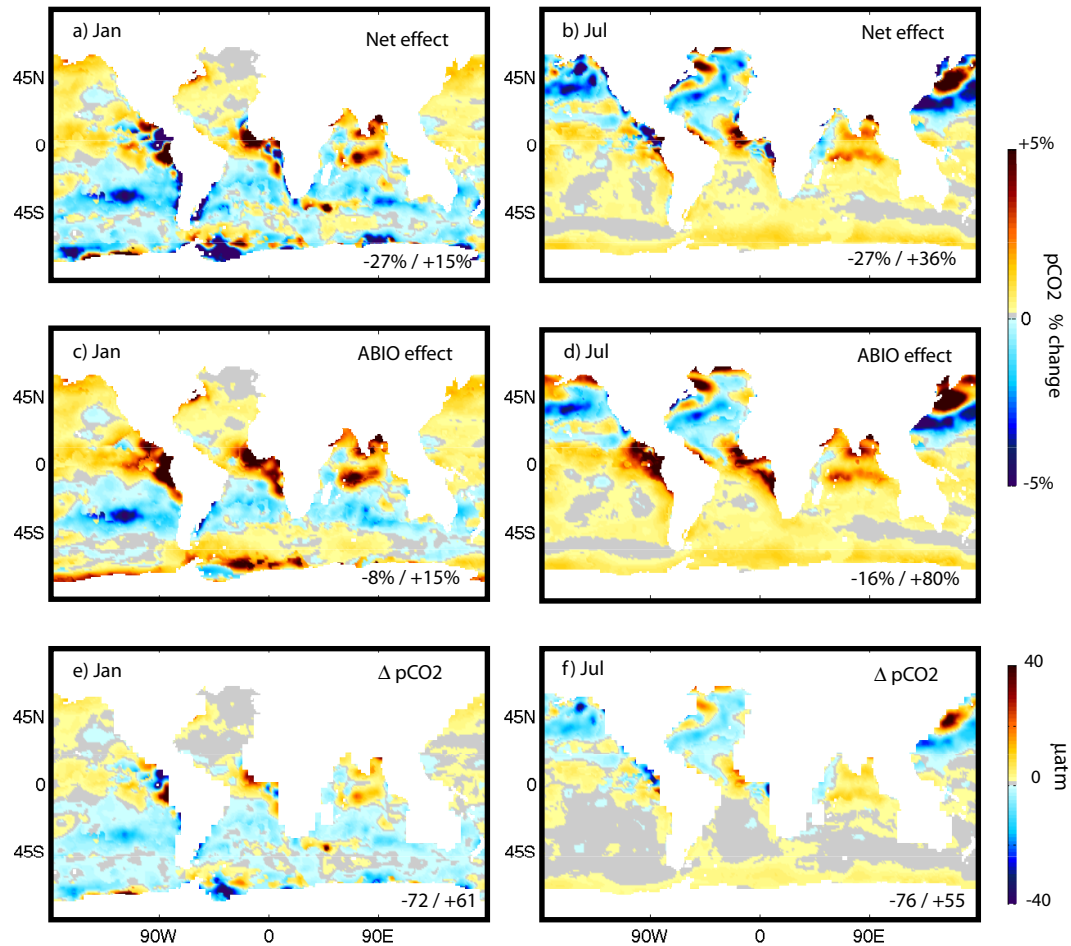


Figure 1. Left and right columns contrast results for January and July. Panels a and b show the net relative change in surface pCO₂, due the sum of various effects in January and July, respectively. Panels c and d show the relative change in pCO₂ due to abiotic effects, i.e. without taking into account BIO, the uptake of DIC by phytoplankton production supported by a NO₃ flux. Panels e and f show the net change in pCO₂ (resulting from all effects) in response to vertical mixing, based on the climatological monthly pCO₂ (Takahashi, et al., 2009). The ABIO (abiotic) effect is the sum of TEM, DIC, ALK and S effects, whereas the net effect comprises the ABIO and BIO effects.

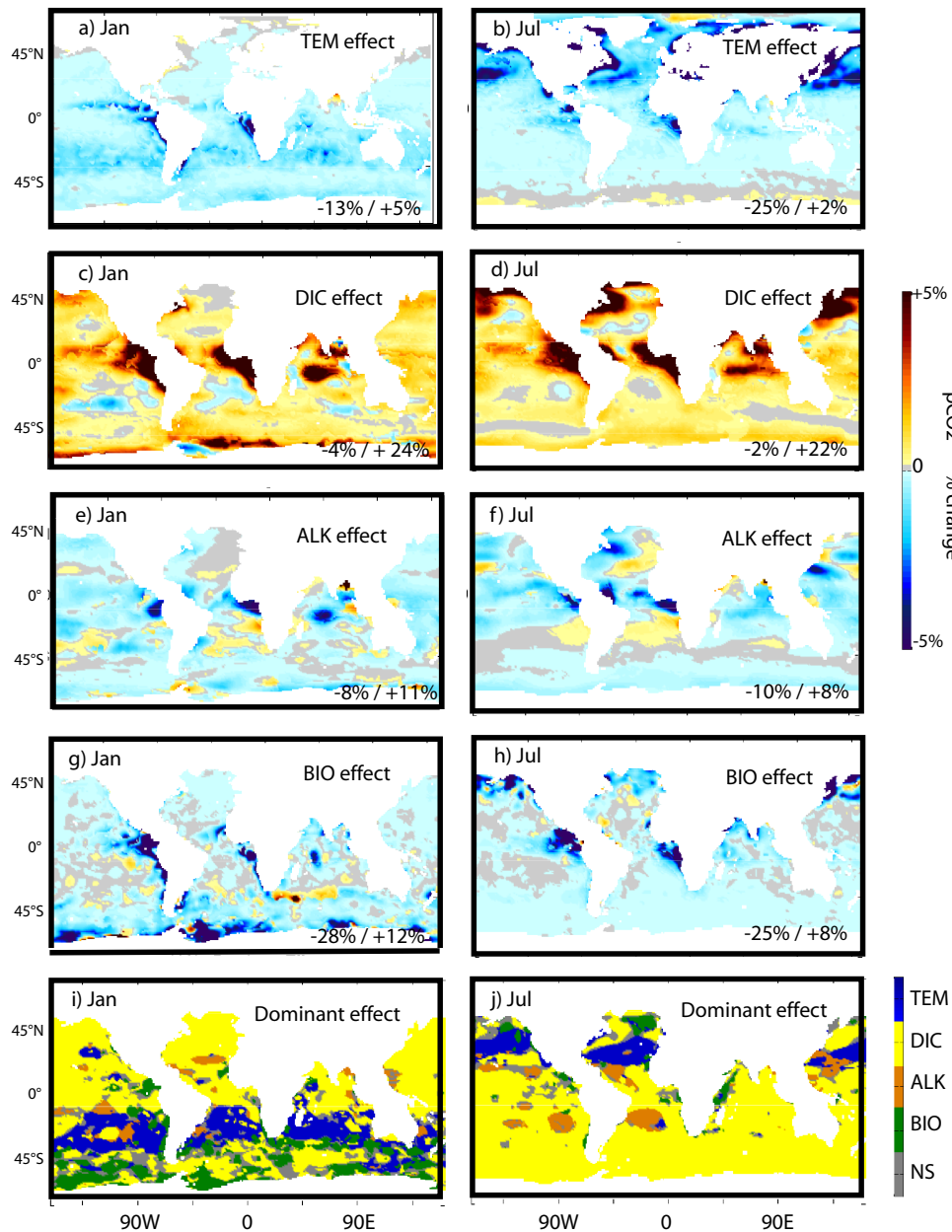


Figure 2. Percent change in surface $p\text{CO}_2$ in response to localized vertical mixing separated in to various factors: (a-b) TEM, (c-d) DIC, (e-f) ALK, (g-h) BIO, i.e. biological uptake due to inputs of NO_3 . For panels a to h the range of results in presented in the lower right section of each panel. The lowermost panels, (i-j), indicate which of these factors has the largest influence on surface $p\text{CO}_2$; ‘NS’ indicates the factor is not significant because it is overrun by opposing influences. These effects are estimated for January (left column) and July (right column). TEM and BIO would lower surface $p\text{CO}_2$, whereas DIC would enhance surface $p\text{CO}_2$. ALK may have either sign. Each of the effects becomes stronger in regions experiencing summer. These estimates are for a vertical diffusivity of $10^{-3} \text{m}^2 \text{s}^{-1}$ acting at the base of the mixed layer for a day, but stronger/weaker mixing would result in a proportionally higher/lower perturbation in $p\text{CO}_2$.

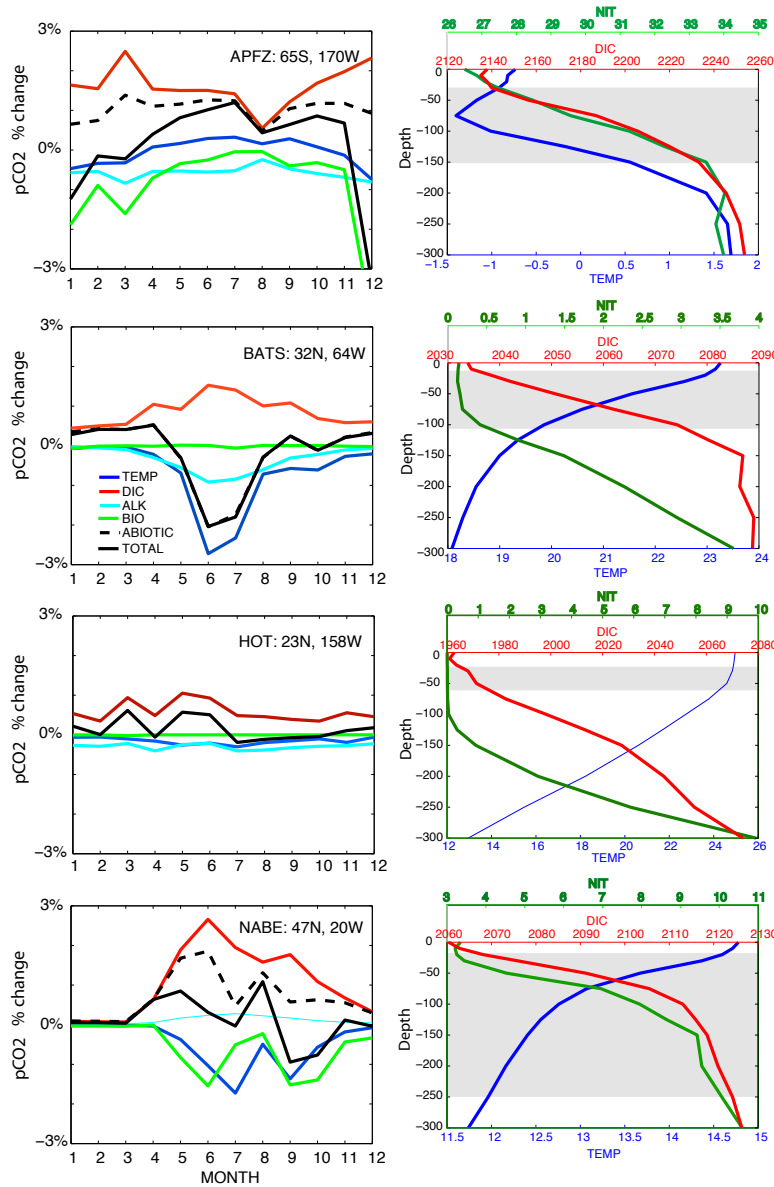


Figure 3. The results are contrasted amongst various oceanic regions through time-series and profiles averaged over a $5^{\circ} \times 5^{\circ}$ region centered on the Antarctic Polar Frontal Zone (APFZ at 65S, 170W), Bermuda Atlantic Time Series (BATS at 32N, 64W), Hawaii Ocean Time series (HOT at 23N, 158W) and the site of the North Atlantic Bloom Experiment (NABE at 47N, 20W). Left column: Annual monthly time series showing the relative change in surface pCO₂ arising from the upwelling/mixing related effects of TEMP, DIC, ALK, BIO, the total abiotic component ABIO, and the net sum of all effects. Positive/negative values indicate the potential for a relative increase/decrease in surface pCO₂, due to mixing represented by $\kappa = 10^{-3} \text{m-s}^{-2}$ acting at the base of the mixed layer for one day. Right column: Annual mean vertical profiles of temperature (deg. C), DIC ($\mu\text{mol/l}$) and NO₃ ($\mu\text{mol/l}$) at the same sites from climatological data. The range in MLD over the annual cycle is shaded grey.